Journal of Materials Chemistry C

ARTICLE

Acid-protected Eu(III) coordination nanoparticles covered with polystyrene†

Hiromitsu Onodera,[ab] Yuichi Kitagawa,[b] Takayuki Nakanishi,[b] Koji Fushimi,[b] and Yasuchika Hasegawa*[b]

Acid-protected Eu(III) coordination nanoparticles composed of Eu(III) complexes, joint ligands, terminate ligands and protected layer are reported. Prepaered acid-protected Eu(III) coordination nanoparticles $[Eu(hfa)_3(dpbp)_x(SDPO)_y]_n$-PS and Eu(III) coordination nanoparticles $[Eu(hfa)_3(dpbp)_x(SDPO)_y]_n$ were characterrized using ESI-Mass spectrometry (ESI-MS), X-Ray diffraction (XRD), Scanning electron microscopy (SEM), dynamic light scattering (DLS) measurements, and termogravimetric analysis (TGA). The $[Eu(hfa)_3(dpbp)_x(SDPO)_y]_n$-PS shows effectively acid-resistance property based on polystyrene layer on their nanoparticle surface. The emission intensity is kept under 3000s in acidic condition (pH = 0.92). In this study, acid-protected Eu(III) coordination nanoparticles are demonstrated.

Introduction

Lanthanide complexes with narrow emission bands and long emission lifetimes have been regarded as attractive luminescent materials for use in electroluminescent optical materials,[1] organic light-emitting diodes(OLEDs),[2] and luminescent bio-sensing applications.[3] At the present stage, various types of luminescent lanthanide complexes have been reported.[4] Lanthanide coordination polymer composed of lanthanide ions and organic joint ligands are also focused for new luminescent materials,[5] recently. Their tight packing structures promote effective thermo-stability and small non-radiative rate constant for strong luminescence. Our research group have reported thermostable lanthanide coordination polymers composed of lanthanide ions and organo-phosphine oxides (decomposition temperature > 300 °C). The lanthanide coordination polymers exhibit high emission quantum yield (quantum yield = 83 %).[6] The thermostable lanthanide coordination polymers are expected to be promising candidates for practical opto-electric devises and temperature-sensitive dyes. In particular, temperature-sensitive dyes under 300 °C are used for temperature distribution measurements of material surfaces such as an aerospace plane in wind tunnel experiments.[7]

The lanthanide coordination polymers with tight-stacking structures, however, lead to formation of insoluble compounds, micro-sized particles, in water and organic solvents. The insoluble micro-sized particles cause multiple light scattering in UV-Vis region. The nanoparticles of lanthanide coordination polymers without multiple light scattering may increase transmission of optical and luminescent materials. We recently successfully reported that luminescent nanoparticles of lanthanide coordination polymers are prepared by addition of monodentate phosphine oxide (triphenyl phosphine oxide: TPPO) as a polymerization terminator.[8]

In order to improve for practical material applications, surface protection on the lanthanide coordination nanoparticles should be required for acidic condition of industrial manufacturing process. Generally, industrial plastic materials are prepared with acid generator such as benzoyl peroxide under water. The presence of H+ source in polymer material results in decomposition of lanthanide coordination nanoparticles under moisture. The acid-protection on the lanthanide coordination nanoparticles expected to be achieved by encapsulation technique using glass materials. Hongshang has demonstrated luminescent Eu3+ chelate nanoparticles covered with octyltrimethoxysilane for encaplsulation.[9] Fukuda has reported lanthanide complexes encapsulated with sol-gel glass.[10] Silica glass or materials are, however, decomposed under acidic condition. Encapsulation using organic polymer attached on the lanthanide coordination nanoparticles may be the most favourable for luminescent materials under moisture.

Here, we have attempted to introduce terminator ligands with vinyl group on the surface of lanthanide coordination nanoparticles. The vinyl groups of terminator ligands, diphenyl(p-vinylphenyl)phosphine oxide (SDPO),[11] can promote polymerization for surface protection under acidic condition(Fig. 1a). The size-controlled nanoparticles are obtained by the reaction of $Eu(hfa)_3(H_2O)_2$ (hfa:

a. *Laser Systems Inc, 1-4-1-10 Nijyuyonken, Nishi-ku, Sapporo, Hokkaido, 063-0801, Japan.*
b. *Faculty School of Engineering, Hokkaido University,North-13 West-8, Kita-ku,Sapporo, Hokkaido 060-8628, Japan. E-mail: hasegaway@eng.hokudai.ac.jp*

hexafluoroacetylacetonate) with joint ligands (dpbp:4,4'-bis(diphenylphosphoryl)biphenyl) and terminator ligands (SDPO) ([Eu(hfa)$_3$(dpbp)$_x$(SDPO)$_y$]$_n$). The Acid-protected Eu(III) coordination nanoparticles are perpared by the polymerization of [Eu(hfa)$_3$(dpbp)$_x$(SDPO)$_y$]$_n$ with styrene monomers under 80 °C ([Eu(hfa)$_3$(dpbp)$_x$(SDPO)$_y$]$_n$-PS (PS : polystyrene, Fig. 1b).

[Eu(hfa)$_3$(dpbp)$_x$(SDPO)$_y$]$_n$ and [Eu(hfa)$_3$(dpbp)$_x$(SDPO)$_y$]$_n$-PS were characterized using ESI-MS, XRD, SEM, DLS measurements, and TGA. The decomposition temperatures of [Eu(hfa)$_3$(dpbp)$_x$(SDPO)$_y$]$_n$ and [Eu(hfa)$_3$(dpbp)$_x$(SDPO)$_y$]$_n$-PS from TGA were determined to be 236 °C and 250 °C, respectively. Emission properties of [Eu(hfa)$_3$(dpbp)$_x$(SDPO)$_y$]$_n$ and [Eu(hfa)$_3$(dpbp)$_x$(SDPO)$_y$]$_n$-PS were estimated using emission spectra, excitation spectra, diffuse reflection spectra and emission lifetimes. We have successfully observed effective acid-resistant ability of [Eu(hfa)$_3$(dpbp)$_x$(SDPO)$_y$]$_n$-PS for practical use under moisture condition. In this study, acid-protected Eu(III) coordination nanoparticles are demonstrated for the first time.

Experimental

Materials

Europium acetate monohydrate (99.9 %) and Styrene monomer(> 99 %), Diphenyl(p-vinylphenyl)phosphine (> 97%) were purchased from Wako Pure Chemical Industries Ltd. 1,1,1,5,5,5-Hexafluoro-2,4-pentanedione, 4,4'-dibromobiphenyl (> 98 %) and Potassium Peroxymonosulfate [> 45%(T) as KHSO$_5$] were obtained from Tokyo Kasei Organic Chemicals. All other chemicals and solvents were reagent grade and were used without further purification.
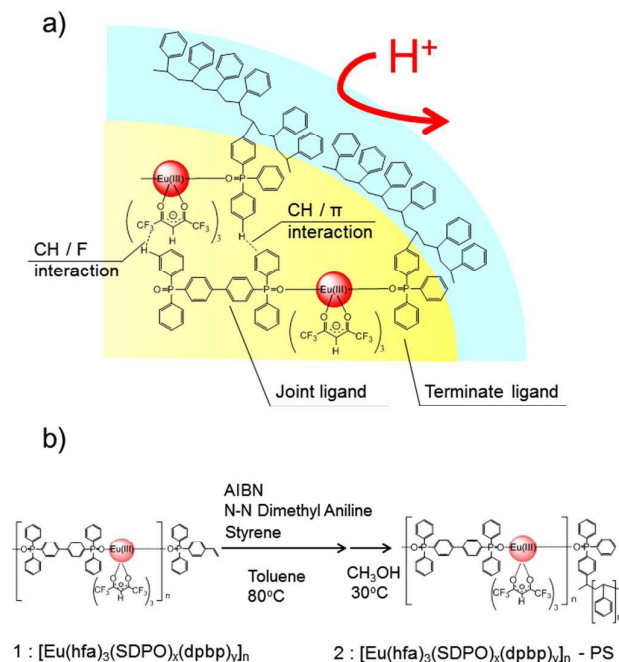

Fig. 1 Preparation scheme of acid protected lanthanide coordination nanoparticles covered with polystyrene.

Apparatus

Infrared spectra were recorded with a JASCO FTIR-350 spectrometer. ^{1}H NMR (400 MHz) spectra were recorded with a JEOL ECS400 spectrometer. Chemical shifts are reported in ppm and are referenced to an internal tetramethylsilane standard for ^{1}H NMR spectroscopy. Elemental analyses were performed with a Yanaco CNH MT-6 analyzer. Thermogravimetric analysis (TGA) was performed on a SEIKO EXSTAR 6000 (TG-DTA 6300). Size-distributions were measured with a BECKMAN COULTER Delsa Nano HC. Scanning electron microscopy (SEM) was performed by JEOL JSM-6510LA (acceleration voltage, 15 kV). Mass spectrometry was performed with a JEOL JMS-T100LP. X-ray photoelectron spectroscopy (XPS) was performed with a JPS-9200 using unmonochromatized Al Kα X-ray.

Preparation of Tris(hexafluoroacetylacetonato)europium Dihydrate [Eu(hfa)$_3$(H$_2$O)$_2$]

Europium acetate monohydrate (5.0 g, 13 mmol) was dissolved in distilled water (20 mL) in a 100 mL flask. A solution of1,1,1,5,5,5-hexafluoro-2,4-pentanedione (7.0 g, 34 mmol) was added dropwise to the solution. The reaction mixture produced a white-yellow precipitate after stirring for 3h at room temperature. The powder was collected by filtration and recrystallized from methanol/water to afford colorless needle crystals of the title compound, yield 9.6 g (95 %). IR (KBr): 1650 (s, C=O), 1145–1258 (s, C–F) cm^{-1}. Anal. Calcd for C$_{15}$H$_7$EuF$_{18}$O$_8$: C, 22.48 %; H, 0.88 %; found: C, 22.12 %; H, 1.01 %.

Preparation of 4,4'-bis(diphenylphosphoryl)biphenyl [dpbp]

4,4'-bis(diphenylphosphoryl)- biphenyl was synthesized according to the published procedure.[6] A solution of n-BuLi (9.3 mL, 1.6 M hexane, 15 mmol), was added dropwise to a solution of 4,4'-dibromobiphenyl (1.9 g, 6.0 mmol) in dry THF (30 mL) at -80°C. The addition was completed in ca. 15 min during which time a yellow precipitate was formed. The mixture was allowed to stir for 3h at -10 °C, after which a PPh$_2$Cl (2.7 mL, 15 mmol) was added dropwise at -80 °C. The mixture was gradually brought to room temperature, and stirred for 14h. The product was extracted with ethyl acetate, the extracts washed with brine for three times and dried over anhydrous MgSO$_4$. The solvent was evaporated, and resulting residue was washed with acetone and ethanol for several times. The obtained white solid and dichloromethane (ca. 40 mL) were placed in a flask. The solution was cooled to 0 °C and then 30 % H$_2$O$_2$ aqueous solution (5 mL) was added to it. The reaction mixture was stirred for 2h. The product was extracted with dichloromethane, the extracts washed with brine for three times and dried over anhydrous MgSO$_4$. The solvent was evaporated to afford a white powder. Recrystallization from dichloromethane gave white crystals of the titled compound. Yield: 1.1 g (33 %). IR(KBr): 1120 (st, P=O) cm^{-1}.^{1}H NMR (400 MHz, CDCl$_3$, 25 °C) δ7.67-7.80 (m, 16H; P-C$_6$H$_5$, C$_6$H$_4$), 7.45-7.60 (m, 12H; P-C$_6$H$_5$, C$_6$H$_4$) ppm. MS(ESI) found: m/z = 555.2, calcd for C$_{36}$H$_{29}$O$_2$P$_2$: [M+H]$^+$, 555.2. Anal. Calcd for

$C_{36}H_{28}O_2P_2$: C, 77.97 %; H, 5.09 %. Found: C,77.49 %; H, 5.20 %.

Preparation of Diphenyl(p-vinylphenyl)phosphine Oxide [SDPO]

Diphenyl(p-vinylphenyl)phosphine Oxide (SDPO) was synthesized according to the published procedure.[12] Diphenyl(p-vinylphenyl)phosphine (5 g, 17.4 mmol) was dissolved in dichloromethane (100 mL) in a 300 mL flask. A saturated aqueous solution of Oxone (21.4 g, 34.8 mmol) and methanol(20 mL) were added to the mixture. The mixture stirred for 3h. The product was extracted with dichloromethane, the extracts washed with brine for three times and dried over anhydrous $MgSO_4$. The solvent was evaporated, and resulting residue was washed with cyclohexane for several times. ^1H NMR (400 MHz, $CDCl_3$, 25 ^oC) δ7.46-7.70 (m, 14H; P-C_6H_5, C_6H_4), 6.71 (dd, 1H; CH), 5.84 (d, 1H; CH_2), 5.37 (d, 1H; CH_2) ppm. MS(ESI) found: m/z = 327.1, calcd for $C_{20}H_{17}OPNa$: [SDPO+Na]$^+$, 327.1. Anal. Calcd for $C_{20}H_{17}OP$: C, 78.93 %; H, 5.63 %. Found: C, 77.30 %; H, 5.64 %.

Preparation of nanoparticles composed of lanthanide coordination polymers [Eu(hfa)$_3$(SDPO)$_x$(dpbp)$_y$]$_n$

Amount of Bidantate dpbp ligands in [Eu(hfa)$_3$(SDPO)$_x$(dpbp)$_{1-x}$]$_n$ (x : molecular ratio of dpbp) was controlled under 0.70(70 %). In the molecular ratio of [Eu(hfa)$_3$(SDPO)$_{0.70}$(dpbp)$_{0.30}$]$_n$, bidantate dpbp ligands (204 mg, 0.37 mmol) and monodantate SDPO ligands (262 mg, 0.86 mmol) were dissolved in methanol (25 mL) in a 50 mL flask. Methanol solution (10 mL) of Eu(hfa)$_3$(H$_2$O)$_2$ (1 g, 1.23 mmol) was added at room temperature. The reaction mixture was stirred for 6h. The product was centrifuged at 4000 rpm for 20 minutes and the white powder of nanoparticles composed of Eu(hfa)$_3$(H$_2$O)$_2$, dpbp and SDPO were prepared. Nanoparticles composed of lanthanide coordination polymers were washed twice with methanol, and then dried. MS(ESI) found: m/z = 1425.2, calcd for $C_{66}H_{47}EuF_{12}O_7P_3$: [Eu(hfa)$_2$(dpbp)(SDPO)]$^+$,1425.2, found: m/z = 1633.2, calcd for $C_{71}H_{49}EuF_{18}O_9P_3$: [Eu(hfa)$_3$(dpbp)(SDPO)+H]$^+$,1633.1.

Preparations of Eu(III) coordination nanoparticles covered with polystyrene

The Eu(III) coordination nanoparticles of [Eu(hfa)$_3$(SDPO)$_x$(dpbp)$_y$]$_n$ (100 mg), AIBN (azobis(isobutyronitrile))(2.2 mg, 13.4 μmol) and were mixed in toluene (10 mL) in a 50 mL flask. The mixture was allowed to stir for 1h at 80 ^oC, after which a styrene monomer (1 mL, 8.7 mmol) was injected by syringe. The reaction mixture was stirred for 2h at 80 ^oC and then was cooled to room temperature. The reaction mixture was added into the methanol(50mL).The solvent was evaporated, and resulting residue was washed with hexane for several times. MS(ESI) found: m/z = 1199.2, calcd for $C_{44}H_{33}EuF_{18}O_7P$: [Eu(hfa)$_3$(SDPO)(PS)$_1$+H]$^+$, 1199.1, found: m/z = 1407.1, calcd for $C_{60}H_{49}EuF_{18}O_7P$: [Eu(hfa)$_3$(SDPO)(PS)$_3$+H]$^+$, 1407.2, found: m/z = 2240.0, calcd for $C_{124}H_{113}EuF_{18}O_7P$: [Eu(hfa)$_3$(SDPO)(PS)$_{11}$+H]$^+$, 2239.7, found: m/z = 2447.9, calcd for $C_{140}H_{129}EuF_{18}O_7P$: [Eu(hfa)$_3$(SDPO)(PS)$_{13}$+H]$^+$, 2447.8, found: m/z = 2677.9,

calcd for $C_{156}H_{144}EuF_{18}O_7PNa$: [Eu(hfa)$_3$(SDPO)(PS)$_{15}$+Na]$^+$, 2677.9, found: m/z = 2864.2, calcd for $C_{172}H_{161}EuF_{18}O_7P$: [Eu(hfa)$_3$(SDPO)(PS)$_{17}$+H]$^+$, 2864.1, found: m/z = 3510.1, calcd for $C_{220}H_{208}EuF_{18}O_7PNa$: [Eu(hfa)$_3$(SDPO)(PS)$_{23}$+Na]$^+$, 3510.4 (PS : unit of polystyrene).

Optical Measurements

Emission, excitation and diffuse reflection spectra of [Eu(hfa)$_3$(dpbp)$_x$(SDPO)$_y$]$_n$ and [Eu(hfa)$_3$(dpbp)$_x$(SDPO)$_y$]$_n$-PS were measured with a JASCO V-670 spectrophotometer and JASCO F-6300-H spectrometer which corrected for the response of the detector system for spectral correction system of optical measurement. The emission lifetimes of the luminescent nanoparticles (powder) were measured by using the third harmonic (355 nm) of a Q-switched Nd:YAG laser [Spectra Physics, INDI-50, full width at half maximum (fwhm) = 5 ns, λ = 1064 nm] and a photomultiplier (Hamamatsu photonics, R5108, response time 1.1 ns). The Nd:YAG laser response was monitored with a digital oscilloscope (Sony Tektronix, TDS3052, 500 MHz) synchronized to the single pulse excitation. The emission lifetimes were determined from the slope of logarithmic plots of the decay profiles. The emission quantum yields of [Eu(hfa)$_3$(dpbp)$_x$(SDPO)$_y$]$_n$ and [Eu(hfa)$_3$(dpbp)$_x$(SDPO)$_y$]$_n$-PS (powders) exited at 370 nm were estimated using a JASCO F-6300-H spectrometer. The photophysical properties of the [Eu(hfa)$_3$(dpbp)$_x$(SDPO)$_y$]$_n$ and [Eu(hfa)$_3$(dpbp)$_x$(SDPO)$_y$]$_n$-PS in the solid-state were investigated from estimation of the 4f-4f emission quantum yields (Φ_{Ln}), and the radiative (k_r) and non radiative (k_{nr}) rate constants from the radiative(τ_{rad}) and observed lifetimes (τ_{obs}). The radiative and observed lifetimes are expressed by

$$\tau_{rad} = \frac{1}{k_r}$$

$$\tau_{obs} = \frac{1}{k_r + k_{nr}}$$

Φ_{Ln}, k_r and k_{nr} of the [Eu(hfa)$_3$(dpbp)$_x$(SDPO)$_y$]$_n$ and [Eu(hfa)$_3$(dpbp)$_x$(SDPO)$_y$]$_n$-PS are given by

$$\Phi_{Ln} = \frac{k_r}{k_r + k_{nr}} = \frac{\tau_{obs}}{\tau_{rad}}$$

$$\frac{1}{\tau_{rad}} = A_{MD,0}n^3\left(\frac{I_{tot}}{I_{MD}}\right)$$

$$k_r = \frac{1}{\tau_{rad}}$$

$$k_{nr} = \frac{1}{\tau_{obs}} - \frac{1}{\tau_{rad}}$$

Where $A_{MD,0}$ is the spontaneous emission probability for the $^5D_0-^7F_1$ transition in *vacuo* (14.65 s^{-1}), n is the refractive index of the medium (an average index of refraction equal to 1.5 was employed), and (I_{tot} / I_{MD}) is the ratio of the total area of the corrected Eu(III) emission spectrum to the area of the $^5D_0$-$^7F_1$ band.

Estimation of acid-resistant properties

Acid-resistant properties of [Eu(hfa)$_3$(dpbp)$_x$(SDPO)$_y$]$_n$ and [Eu(hfa)$_3$(dpbp)$_x$(SDPO)$_y$]$_n$-PS were estimated by change of emission intensity under acidic condition. The amount (5 mg)

of $[Eu(hfa)_3(dpbp)_x(SDPO)_y]_n$ and $[Eu(hfa)_3(dpbp)_x(SDPO)_y]_n$-PS were dispersed in ethanol (2 mL), and then 12 % nitric acid (100 μL) was added. The decomposition processes are observed using emission spectra of $[Eu(hfa)_3(dpbp)_x(SDPO)_y]_n$ and $[Eu(hfa)_3(dpbp)_x(SDPO)_y]_n$-PS exited at 370 nm (JASCO F-6300-H spectrometer). The decomposition indexes are calculated using the emission intensity at 613 nm (for 0-4000s).

Results and discussion

Structural characterizations

The structures of prepared $[Eu(hfa)_3(dpbp)_x(SDPO)_y]_n$ and $[Eu(hfa)_3(dpbp)_x(SDPO)_y]_n$-PS were characterized using powder XRD measurements. These XRD spectra are shown in Figure 2a. Peaks for $[Eu(hfa)_3(dpbp)_x(SDPO)_y]_n$ were observed at 7.59^o, 8.85^o, 9.46^o, 20.13^o, 20.65^o and 21.45^o. Peaks for $[Eu(hfa)_3(dpbp)_x(SDPO)_y]_n$-PS were also observed at 7.59^o, 8.85^o, 9.46^o, 20.13^o, 20.65^o and 21.45^o, which are the same as those for $[Eu(hfa)_3(dpbp)_x(SDPO)_y]_n$. The 2θ diffraction peaks of $[Eu(hfa)_3(dpbp)_x(SDPO)_y]_n$ and $[Eu(hfa)_3(dpbp)_x(SDPO)_y]_n$-PS were similar to the corresponding peaks for previously reported $[Eu(hfa)_3(dpbp)]_n$.[6] These results indicate that the geometrical structures of nanoparticles are the same as those of $[Eu(hfa)_3(dpbp)]_n$ (see supporting information Fig. S1).

Polystyrene on the nanoparticle surface was observed using ESI-MS. This result indicates formation of $[Eu(hfa)_3(dpbp)_x(SDPO)_y]_n$ covered with amorphous polystyrene. Unfortunately, we did not observed effective IR-signal of polystyrene thin layer on the nanoparticles (see supporting information Fig. S2).

Quantitative analysis of carbon in $[Eu(hfa)_3(dpbp)_x(SDPO)_y]_n$ and $[Eu(hfa)_3(dpbp)_x(SDPO)_y]_n$-PS were carried out using X-ray photoelectron spectra (XPS). The XPS of C1s, Eu3d5/2, and F1s were shown in supporting information Fig. S3. The atomic ratio of carbon in $[Eu(hfa)_3(dpbp)_x(SDPO)_y]_n$ and $[Eu(hfa)_3(dpbp)_x(SDPO)_y]_n$-PS using C1s and F1s spectra were found to be 3.0 and 11.1, respectively. The atomic ratio in $[Eu(hfa)_3(dpbp)_x(SDPO)_y]_n$-PS is 3.7 times larger than that in $[Eu(hfa)_3(dpbp)_x(SDPO)_y]_n$. We consider that $[Eu(hfa)_3(dpbp)_x(SDPO)_y]_n$-PS are covered with large amount of polystyrene layer.

The thermal stability of $[Eu(hfa)_3(dpbp)_x(SDPO)_y]_n$ and $[Eu(hfa)_3(dpbp)_x(SDPO)_y]_n$-PS were evaluated using TGA (Fig. 2b). The Eu(III)-nanoparticle $[Eu(hfa)_3(dpbp)_x(SDPO)_y]_n$ and $[Eu(hfa)_3(dpbp)_x(SDPO)_y]_n$-PS show two decomposition temperatures. The first decomposition temperatures of $[Eu(hfa)_3(dpbp)_x(SDPO)_y]_n$ and $[Eu(hfa)_3(dpbp)_x(SDPO)_y]_n$-PS found to be 236 ^oC and 250 ^oC, respectively. The first decomposition temperatures are due to elimination of terminator ligands(SDPO) and polystyrene. The second decomposition temperatures for Eu(III)-nanoparticle $[Eu(hfa)_3(dpbp)_x(SDPO)_y]_n$ and $[Eu(hfa)_3(dpbp)_x(SDPO)_y]_n$-PS found to be 316 ^oC and 314 ^oC, respectively. The second decomposition temperatures are agree well with that of standard coordination polymer $[Eu(hfa)_3(dpbp)]_n$ (see supporting information Fig. S4).
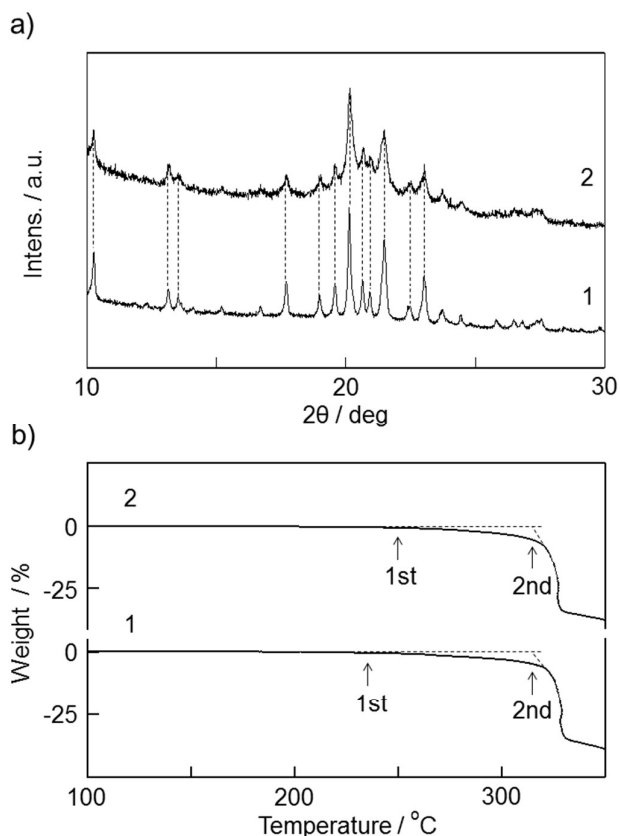

Fig. 2 a) XRD patterns of **1:** $[Eu(hfa)_3(dpbp)_x(SDPO)_y]_n$ and **2:** $[Eu(hfa)_3(dpbp)_x(SDPO)_y]_n$-PS.   b) TGA curves of **1:** $[Eu(hfa)_3(dpbp)_x(SDPO)_y]_n$ and **2:** $[Eu(hfa)_3(dpbp)_x(SDPO)y]_n$-PS in argon atmosphere at a heating rate of 2 ^oC min^{-1}.
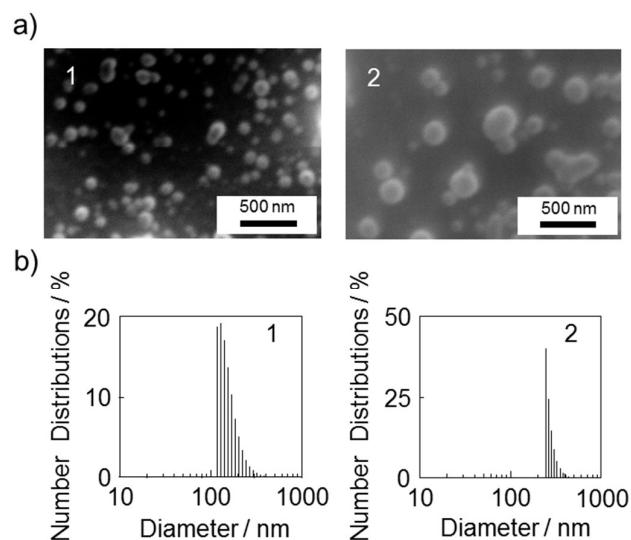
Fig. 3 a) SEM images of **1:** $[Eu(hfa)_3(dpbp)_x(SDPO)_y]_n$ and **2:** $[Eu(hfa)_3(dpbp)_x(SDPO)_y]_n$-PS.   b) Number distributions of **1:** $[Eu(hfa)_3(dpbp)_x(SDPO)_y]_n$ and **2:** $[Eu(hfa)_3(dpbp)_x(SDPO)_y]_n$-PS using DLS measurements.

The SEM images of $[Eu(hfa)_3(dpbp)_x(SDPO)_y]_n$ and $[Eu(hfa)_3(dpbp)_x(SDPO)_y]_n$-PS are shown in Fig. 3a. We found sphere shape of nanoparticles. The particle size distribution of $[Eu(hfa)_3(dpbp)_x(SDPO)_y]_n$ and $[Eu(hfa)_3(dpbp)_x(SDPO)_y]_n$-PS were characterized using DLS measurements. These size distributions are shown in Fig. 3b (scattering intensities of DLS measurement: see supporting information Fig. S5). The maximum distributions of $[Eu(hfa)_3(dpbp)_x(SDPO)_y]_n$ and $[Eu(hfa)_3(dpbp)_x(SDPO)_y]_n$-PS are estimated to be 156.7 nm and 272.9 nm, respectively. We observed increase of particle size of $[Eu(hfa)_3(dpbp)_x(SDPO)_y]_n$-PS for formation of amorphous polystyrene thin layers on the $[Eu(hfa)_3(dpbp)_x(SDPO)_y]_n$ surface.

Emission properties

The emission spectra of $[Eu(hfa)_3(dpbp)_x(SDPO)_y]_n$ and $[Eu(hfa)_3(dpbp)_x(SDPO)_y]_n$-PS in the solid-state are shown in Fig. 4a. Emission bands of $[Eu(hfa)_3(dpbp)_x(SDPO)_y]_n$ and $[Eu(hfa)_3(dpbp)_x(SDPO)_y]_n$-PS excited at 370 nm were observed at 578, 592, 613, 650 and 698 nm, and are attributed to the 4f–4f transitions of $^5D_0–^7F_J$ with J = 0, 1, 2, 3 and 4, respectively. The emission spectra were normalized with respect to the magnetic dipole transition intensities at 592 nm (Eu(III):$^5D_0–^7F_1$), which are known to be insensitive to the surrounding environment of the lanthanide ions. The decrease in the emission intensity of $[Eu(hfa)_3(SDPO)_x(dpbp)_y$-PS$]_n$ is caused by the polystyrene layer on the surface of Eu(III) coordination nanoparticles.

Fig. 4b and c show excitation and diffuse reflection spectra for $[Eu(hfa)_3(dpbp)_x(SDPO)_y]_n$ and $[Eu(hfa)_3(dpbp)_x(SDPO)_y]_n$-PS in solid state at room temperature. The unit of diffuse reflection spectra (Fig. 4c) is Kubelka-Munk (KM), which is depends on the surface of the materials. The excitation and KM intensity of $[Eu(hfa)_3(SDPO)_x(dpbp)_y$-PS$]_n$ increases in comparison with $[Eu(hfa)_3(dpbp)_x(SDPO)_y]_n$. This phenomenon is caused by polymerization of polystyrene on the surface of Eu(III) coordination nanoparticles. The increased absorbance bands of $[Eu(hfa)_3(SDPO)_x(dpbp)_y$-PS$]_n$ from 340nm to 450nm drived from hfa ligands, because the absorbance bands of the polystyrene are less than 300nm. We consider that increased absorbance bands of $[Eu(hfa)_3(SDPO)_x(dpbp)_y$-PS$]_n$ are caused by interaction between hfa ligands and polystyrene. The specific absorbance bands are similar to a ILCT (inter-ligand charge transfer) band of hfa ligands in the solid-state.[13]

Fig. 5 show time-resolved emission decay profiles for $[Eu(hfa)_3(dpbp)_x(SDPO)_y]_n$ and $[Eu(hfa)_3(dpbp)_x(SDPO)_y]_n$-PS in the solid-state. The emission lifetimes were determined from the slopes of the logarithmic plots of the decay profiles. The emission decay of $[Eu(hfa)_3(dpbp)_x(SDPO)_y]_n$ (Fig. 5a) and $[Eu(hfa)_3(dpbp)_x(SDPO)_y]_n$-PS (Fig. 5b) have one component (0.66 ± 0.01 ms and 0.64 ± 0.01 ms).

The emission life times are similar to that of pervious $[Eu(hfa)_3(dpbp)_{0.20}(TPPO)_{0.80}]_n$ ($\tau = 0.66 \pm 0.01$ ms).[8] These
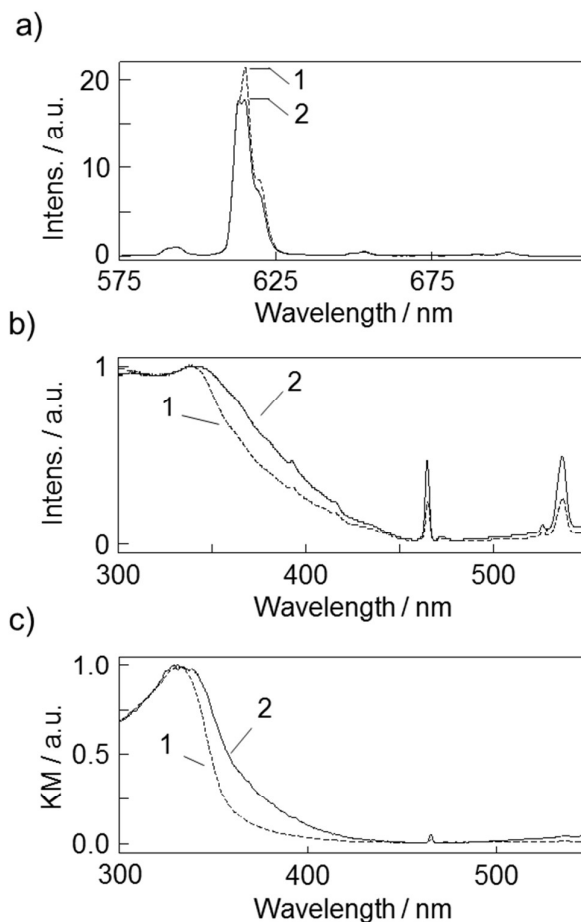

Fig. 4 a) Emission spectra of 1: $[Eu(hfa)_3(dpbp)_x(SDPO)_y]_n$ and 2: $[Eu(hfa)_3(dpbp)_x(SDPO)_y]_n$-PS in solid state at room temperature. Excited at 370 nm. b) Excitation spectra of 1: $[Eu(hfa)_3(dpbp)_x(SDPO)_y]_n$ and 2: $[Eu(hfa)_3(dpbp)_x(SDPO)_y]_n$-PS in solid state at room temperature. Monitored at 613 nm. c) Diffuse reflection spectra of 1: $[Eu(hfa)_3(dpbp)_x(SDPO)_y]_n$ and 2: $[Eu(hfa)_3(dpbp)_x(SDPO)_y]_n$-PS in solid state at room temperature.
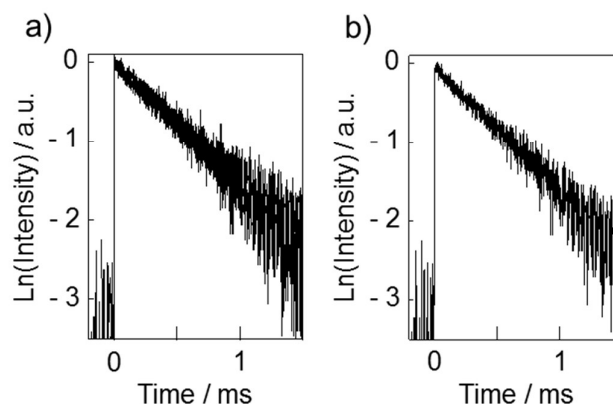
Fig. 5 Emission decays of a): $[Eu(hfa)_3(dpbp)_x(SDPO)_y]_n$ and b): $[Eu(hfa)_3(dpbp)_x(SDPO)_y]_n$-PS in solid state at room temperature excited at 355 nm (third harmonic of a Q-switched Nd:YAG laser: fwhm = 5 ns, λ =1064 nm).

ARTICLE
Journal Name

emission life times are smaller than that of bulk Eu(III) coordination powder $[Eu(hfa)_3(dpbp)]_n$ (τ = 0.91 ± 0.01 ms). The smaller emission lifetimes of $[Eu(hfa)_3(dpbp)_x(SDPO)_y]_n$ and $[Eu(hfa)_3(dpbp)_x(SDPO)_y]_n$-PS may be due to presence of vibrational relaxation on the nanoparticle surface covered with terminate ligands (SDPO).

The intrinsic 4f-4f emission quantum yield of $[Eu(hfa)_3(dpbp)_x(SDPO)_y]_n$ and $[Eu(hfa)_3(dpbp)_x(SDPO)_y]_n$-PS in the solid-state were also determined based on the emission lifetime with a single-exponential decay and 4f-4f transition probability (Table 1).[6] The 4f-4f emission quantum yield (Φ_{Ln}) of $[Eu(hfa)_3(dpbp)_x(SDPO)_y]_n$ and $[Eu(hfa)_3(dpbp)_x(SDPO)_y]_n$-PS are calculated to be 70 % and 63 %, respectively.

Fig. 6 show time dependences of the emission intensities of $[Eu(hfa)_3(dpbp)_x(SDPO)_y]_n$ and $[Eu(hfa)_3(dpbp)_x(SDPO)_y]_n$-PS under the acidic condition (pH = 0.92). We observed effective decrease of the emission intensity of $[Eu(hfa)_3(dpbp)_x(SDPO)_y]_n$ (circle). The emission intensity was found to be 60 % at around 3000s. In contrast, the emission intensity of $[Eu(hfa)_3(dpbp)_x(SDPO)_y]_n$-PS was decreased at 500s (88 %), and then the emission intensity was kept under 3000s (80%, square). The acid resistant property of $[Eu(hfa)_3(dpbp)_x(SDPO)_y]_n$-PS are successfully improved using polystyrene layer composed of SDPO and styrene monomers on the nanoparticles surface.

Table 1 Photophysical properties of $[Eu(hfa)_3(dpbp)_x(SDPO)_y]_n$ and $[Eu(hfa)_3(dpbp)_x(SDPO)_y]_n$-PS in the solid-state.

u(III) nanoparticles	τ_{obs} [a] / ms	τ_{rad} [b] / ms	Φ_{Ln} [c] / %	k_r [d] / S^{-1}	k_{nr} [e] / S^{-1}
$[Eu(hfa)_3(dpbp)_x(SDPO)_y]_n$	0.66	0.94	0.70	1.1×10^3	4.5×10^2
$[Eu(hfa)_3(dpbp)_x(SDPO)_y]_n$-PS	0.64	1.02	0.63	9.8×10^2	5.8×10^2

[a] Observed lifetimes (τ_{obs}) of the Eu(III) coordination nanoparticles were measured by excitation at 355nm(Nd : YAG 3ω). [b] Radiative lifetime τ_{rad} = 1 / $A_{MD,0}$ n^3(I_{tot} / I_{MD}). $A_{MD,0}$ is the spontaneous emission probability for the $^5D_0$-$^7F_1$ transition in *vacuo* (14.65 s^{-1}), n is the refractive index of the medium (an average index of refraction equal to 1.5 was employed[*]), and (I_{tot} / I_{MD}) is the ratio of the total area of the corrected Eu(III) emission spectrum to the area of the $^5D_0$-$^7F_1$ band. [c] 4f-4f emission quantum yields Φ_{Ln} = τ_{obs} / τ_{rad}. [d] Radiative rate constants k_r = 1 / τ_{rad}. [e] Non-radiative rate constants knr = 1 / τ_{obs} − k_r.
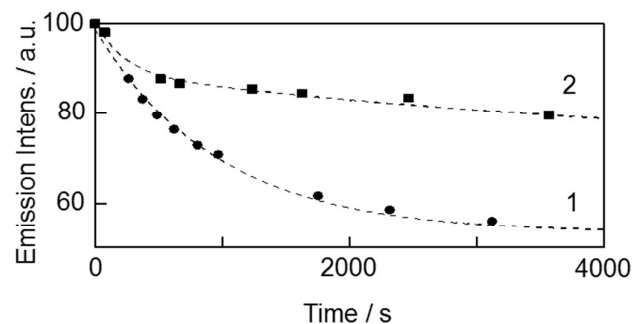

Fig. 6 Time dependences of the emission intensities of **1**: $[Eu(hfa)_3(dpbp)_x(SDPO)_y]_n$ (circles) and **2**: $[Eu(hfa)_3(dpbp)_x(SDPO)_y]_n$-PS (squares) under Acidic condition (pH = 0.92).

Conclusions

We successfully prepared acid-protected Eu(III) coordination nanoparticles covered with polystyrene. The $[Eu(hfa)_3(dpbp)_x(SDPO)_y]_n$-PS are effectively protected by polystyrene layer on their nanoparticle surface. The emission intensity is kept under 3000s in acidic condition (pH = 0.92). Acid-protected Eu(III) coordination nanoparticles may be useful in applications such as temperature-sensitive dyes and luminescent display under high temperature and humidity condition. Recently, we successfully prepared the thin films composed of Eu(III) coordination polymer for EL devices. [14] Polystyrene-coated Eu(III) luminescent nanoparticles are expected to open up new material fields of photo functional organo and metal complexes.

Acknowledgements

References

1 (a) G. Blasse and B. C. Grabmaier, Luminescent Materials, Springer-Verlag, New York, 1994; (b) A. Vogler and H. Kunkely, Luminescent Metal Complexes: Diversity of Excited States, in:Topics in Current Chemistry, vol. 213, Transition Metal and Rare Earth Compounds (Ed.: H. Yersin), Springer-Verlag, New York, 2001.

2 (a) R. Gao, D. G. Ho, B. Hernandez, M. Selke, D. Murphy, P. I. Djurovich and M. E. Thompson, *J. Am. Chem. Soc.,* 2002, **124**, 14828; (b) J. Li, P. I. Djurovich, B. D. Alleyne, M. Yousufuddin, N. N. Ho, J. C. Thomas, J. C. Peters, R. Bau and M. E. Thompson, *Inorg. Chem.,* 2005, **44**, 1713; (c) X.-M. Yu, G.-J. Zhou, C.-S. Lam, W.-Y. Wong, X.-L. Zhu, J.-X. Sun, M. Wong and H.-S. Kwok, *J. Organomet. Chem.,* 2008, **693**, 1528.

3 (a) N. Weibel, L. J. Charbonniere, M. Guardigli, A. Roda and R.Ziessel, *J. Am. Chem. Soc.,* 2004, **126**, 4888; (b) J.-C. G. Bünzli and C. Piguet, *Chem. Soc. Rev.,* 2005, **34**, 1048; (c) S. Faulkner and B. P. Burton-Pye, *Chem. Commun.,* 2005, **259**; (d) J. Yu, D. Parker, R. Pal, R. A. Poole and M. J. Cann, *J. Am. Chem. Soc.,* 2006, **128**, 2294; (e) B. McMahon, P. Mauer, C. P. McCoy, T. C. Lee and T. Gunnlaugsson, *J. Am. Chem. Soc.,* 2009, **131**, 17542.

4 (a) A. Ablet, S.-M. Li, W. Cao, X.-J. Zheng, W.-T. Wong and L.-P. Jin, *Chem. Asian J.,* 2013, **8**, 95; (b) J. Xu, L. Jia, N. Jin, Y. Ma, X. Liu, W. Wu, W. Liu, Y. Tang and F. Zhou, *Chem. Eur. J.,* 2013, **19**, 4556; (c) N. Wartenberg, O. Raccurt, E. Bourgeat-Lami, D. Imbert and M. Mazzanti, *Chem. Eur. J.,* 2013, **19**, 3477; (d) C. Camp, J. Pe´caut and M. Mazzanti, *J. Am. Chem. Soc.,* 2013, **135**, 12101; (e) C. Zhao, Q. –F. Sun, W. M. Hart-Cooper, A. G. DiPasquale, F. D. Toste, R. G. Bergman and K. N. Raymond, *J. Am. Chem. Soc.,* 2013, **135**, 18802; (f) S. Biju, N. Gopakumar, J.-C. G. Bünzli, R. Scopelliti, H. K. Kim and M. L. P. Reddy, *Inorg. Chem.,* 2013, **52**, 8750; (g) D. Sykes, S. C. Parker, I. V. Sazanovich, A. Stephenson, J. A. Weinstein and M. D. Ward, *Inorg. Chem.,* 2013, **52**, 10500; (h) M. L. P. Reddy and S. Sivakumar, *Dalton Trans.,* 2013, **42**, 2663; (i) A. C.

Mendonça, A. F. Martins, A. Melchior, S. M. Marques, S. Chaves, S. Villette, S. Petoud, P. L. Zanonato, M. Tolazzi, C. S. Bonnet, É. Tóth, P. D. Bernardo, C. F. G. C. Geraldesb and M. A. Santos, *Dalton Trans.,* 2013, **42**, 6046; (j) J. W. Walton, A. Bourdolle, S. J. Butler, M. Soulie, M. Delbianco, B. K. McMahon, R. Pal, H. Puschmann, J. M. Zwier, L. Lamarque, O. Maury, C. Andraudb and D. Parker, *Chem. Commun.,* 2013, **49**, 1600; (k) K. L. Gempf, S. J. Butler, A. M. Funk and D. Parker, *Chem. Commun.,* 2013, **49**, 9104; (l) E. R. Trivedi, S. V. Eliseeva, J. Jankolovits, M. M. Olmstead, S. Petoud and V. L. Pecoraro, *J. Am. Chem. Soc.,* 2014, **136**, 1526; (m) A. J. Metherell, W. Cullen, A. Stephenson, C. A. Hunter and M. D. Ward, *Dalton Trans.,* 2014, **43**, 71; (n) E. Debroye, S. V. Eliseeva, S. Laurent, L. V. Elst, R. N. Mullerd and T. N. Parac-Vogt, *Dalton Trans.,* 2014, **43**, 3589; (o) N. J. Rogers, S. Claire, R. M. Harris, S. Farabi, G. Zikeli, I. B. Styles, N. J. Hodges and Z. Pikramenou, *Chem. Commun.,* 2014, **50**, 617.

5   (a) J. Rocha, L. D. Carlos, F. A. A. Paza and D. Ananias, *Chem. Soc. Rev.*, 2011, **40**, 926; (b) C. Daiguebonne, N. Kerbellec, O. Guillou, J.-C. Bunzli, ¨ F. Gumy, L. Catala, T. Mallah, N. Audebrand, Y. G´erault, K. Bernot and G. Calvez, *Inorg. Chem.*, 2008, **47**, 3700; (c) Y. Hasegawa and T. Nakanishi, *RSC Advances,* 2015, **5**, 338.

6   K. Miyata, T. Ohba, A. kobayashi, M. Kato, T. Nakanishi, K. Fushimi and Y. Hasegawa, *ChemPlusChem,* 2012, **77**, 277.

7   K. Miyata, Y. Konno, T. Nakanishi, A. kobayashi, M. Kato, T. Nakanishi, K. Fushimi and Y. Hasegawa, *Angew. Chem. Int.* Ed., 2013, **52**, 6413.

8   H. Onodera, A. Nakajima, T. Nakanishi, K. Fushimi and Y. Hasegawa, *e-J. Surf. Sci. Nanotech.*, 2015, **13**, 219.

9   H. Peng, C. Wu, Y. Jiang, S. Huang, J. McNeill, *Langmuir*, 2007, **23**, 1591.

10 T. Fukuda, S. Kato, E. Kin, K. Okaniwa, H. Morikawa, Z. Honda and N. Kamata, Opt. Mater., 2009, **32**, 22.

11 A. Kusumaatmaja, T. Ando, K. Terada, S. Hirohara, T. Nakashima, T. Kawai, T. Terashima and M. Tanihara, *J. Polym. Sci. Part A: Polym. Chem.,* 2013, **51**(12), 2527.

12 J. Sanmartin, M. R. Bermejo, A. Sousa, M. Fondo, E. Gomez-Forneas and C. McAuliffe, *Acta Chem. Scand.*, 1997, **51**, 59.

13 (a) S. V. Eliseeva, O. V. Kotova, F. Gumy, S. N. Semenov, V. G. Kessler, L. S. Lepnev, J. -C. G. Bünzli, N. P. Kuzmina, *J. Phys. Chem. A*, 2008, **112**, 3614; (b) Y. Hasegawa, R. Hieda, T. Nakagawa, T. Kawai, *Helv. Chim. Acta*, 2009, **92**, 2238; (c) Y. Hasegawa, R. Hieda, K. Miyata, T. Nakagawa, T. Kawai, *Eur. J. Inorg. Chem.*, 2011, **32**, 4978.

14 Y. Hasegawa, T. Sugawara, T. Nakanishi, Y. Kitagawa, M. Takada, A. Niwa, H. Naito and K. Fushimi, *ChemPlusChem,* 2015, inPress (DOI : 10.10021 / cplu. 201500382).

Graphical Abstract

CH / F interaction

CH / π interaction

Joint ligand

Terminate ligand

H+